Title
Cerebroretinal Vasculopathies

Journal
Brain Pathology, 24(5)

ISSN
1015-6305

Authors
Kolar, Grant R
Kothari, Parul H
Khanlou, Negar
et al.

Publication Date
2014-09-01

DOI
10.1111/bpa.12178

Peer reviewed

Brain Pathology ISSN 1015-6305

MINI-SYMPOSIUM: Pathology and Genetics of (non-CAA) Cerebral Microvascular Disease

Neuropathology and Genetics of Cerebroretinal Vasculopathies

Grant R. Kolar[1]; Parul H. Kothari[2]; Negar Khanlou[3]; Joanna C. Jen[4]; Robert E. Schmidt[5]; Harry V. Vinters[3,4]

[1] Department of Pathology, Saint Louis University School of Medicine, [2] Department of Genetics, [5] Division of Neuropathology, Washington University in St. Louis, St. Louis, MO, [3] Departments of Pathology and Laboratory Medicine (Neuropathology), and [4] Neurology, David Geffen School of Medicine, Ronald Reagan UCLA Medical Center, University of California Los Angeles (UCLA), Los Angeles, CA.

Keywords
cerebral microvascular disease, CRV, hereditary endotheliopathy with retinopathy, nephropathy, and stroke, hereditary vascular retinopathy, HERNS, ocular microvascular disease.

Corresponding author:
Grant R. Kolar, MD, PhD, Department of Pathology, Saint Louis University School of Medicine, St. Louis, MO 63104
(E-mail: *kolargr@slu.edu*)

Received 11 July 2014
Accepted 14 July 2014

doi:10.1111/bpa.12178

Abstract

Cerebroretinal vasculopathy (CRV) and the related diseases hereditary endotheliopathy with retinopathy, neuropathy, and stroke (HERNS), hereditary vascular retinopathy (HVR) and hereditary systemic angiopathy (HSA) [subsequently combined as retinovasculopathy and cerebral leukodystrophy (RVCL)] are devastating autosomal-dominant disorders of early to middle-age onset presenting with a core constellation of neurologic and ophthalmologic findings. This family of diseases is linked by specific mutations targeting a core region of a gene. Frameshift mutations in the carboxyl-terminus of three prime exonuclease-1 (TREX1), the major mammalian 3′ to 5′ DNA exonuclease on chromosome 3p21.1-p21.3, result in a systemic vasculopathy that follows an approximately 5-year course leading to death secondary to progressive neurologic decline, with sometimes a more protracted course in HERNS. Neuropathological features include a fibrinoid vascular necrosis or thickened hyalinized vessels associated with white matter ischemia, necrosis and often striking dystrophic calcifications. Ultrastructural studies of the vessel walls often demonstrate unusual multilaminated basement membranes.

INTRODUCTION

History and naming conventions

Cerebroretinal vasculopathy (CRV) was first described in 1988 by Grand *et al* (5) as a unique clinical syndrome with autosomal-dominant inheritance beginning at middle age. These patients had a constellation of neurologic and ophthalmologic findings including retinal vasculopathy visualized on fluorescein angiograms and periventricular white matter lesions in the brain seen by magnetic resonance imaging (MRI). Eight patients spanning three generations were identified in the initial pedigree (5). An additional unrelated Ashkenazi-Jewish family was reported at the same time (5, 22). Subsequently, a separate Ashkenazi-Jewish family (6) and two other families were reported (16, 27). Historically, reports on this cluster of patients highlighted retinal and cerebral manifestations but less prominent systemic manifestations were noted clinically (Grand and Atkinson, unpub. data).

In 1997, Jen *et al* (8) described a family of Chinese descent with 11 affected members spanning three generations who manifested an illness with a similar course to that of CRV (8). Distinct renal disease was noted in these patients in addition to stroke, dementia and retinopathy, the latter all seen in CRV. These patients showed an expanded range of symptoms from their cerebral disease that included migraine and mood disorders. Presenting with a distinctive multiorgan pattern of involvement, it was termed hereditary endotheliopathy with retinopathy, nephropathy and stroke (HERNS) (2). This report was the first to include ultrastructural studies showing distinctive multilaminated vascular basement membranes in the brain, kidney, gastrointestinal tract and skin. Genetic analysis was used to rule out linkage to the cerebral autosomal-dominant arteriopathy with subcortical infarcts and leukoencephalopathy (CADASIL)-locus on chromosome 19 (8).

In 1990, Storimans *et al* (25) (with a follow-up by Terwindt *et al* in 1998 (26)) published a report of a syndrome of retinal vasculopathy, migraines and Raynaud's phenomenon in a Dutch kindred, which they named hereditary vascular retinopathy (HVR). As initially reported, these patients did not appear to have shortened life expectancy, cerebral pseudotumors or severe compromise of visual acuity (caused by predominant peripheral retinal involvement). A whole genome screen in the extended family found linkage to 3p21.1-p21.3 (17) and a genetic analysis of patients from the CRV and HERNS (2) kindreds demonstrated linkage to the same region. Furthermore, a group of frameshift mutations in

the *trex1* gene resulted in truncated three prime exonuclease-1 (TREX-1) proteins in all individuals with these diseases (22).

In 2007, CRV, HERNS and HVR were grouped together as retinal vasculopathy with cerebral leukodystrophy (RVCL, OMIM 192315) (22). Subsequently, a familial disease called hereditary systemic angiopathy (HSA), which bears a remarkable resemblance to RVCL (28), was reported. In this disease, not only are neurological and visual symptoms present in the same age group, but migraine-like headaches, seizures, motor paresis, renal and hepatic dysfunction are seen. Most recently, a report under peer review (as of 2014, Stam, Kothari *et al*) examines the commonalities of most of the known families with these diseases. For simplicity, this report will refer to this disease process predominantly as CRV.

CLINICAL FEATURES AND PRESENTATION

CRV is an autosomal-dominant disorder with 100% penetrance comprised at its root of a vasculopathy that predominantly involves the white matter of brain and the retina. Patients usually present with visual complaints (average age 45) or neurological symptoms (average age of 47). The disease is uniformly fatal within 5–10 years from the time of diagnosis (5, 8, 22). Although the vast majority of patients have a significant progressive neurologic decline leading to their death, superimposed infections (pneumonias, opportunistic infections) and in some cases gastrointestinal (GI) bleed have been the cause of death in many patients after they become debilitated or after steroid treatment. All patients have eye disease at the time of diagnosis, 77% being symptomatic. Only 25% initially present with evidence of neurological symptoms. Within 2–3 years of diagnosis, however, almost all have neurological symptoms (Stam, Kothari, *et al*, unpub. data). A progressive loss of small blood vessels in middle age accounts for both the small multifocal and the large mass lesions of the white matter observed on imaging (Stam, Kothari, *et al*, unpub. data; see radiology and pathology discussions to follow). While vascular lesions in the retina and cerebral white matter are present in every patient and almost always dominate the clinical course, a systemic vasculopathy probably occurs as evidenced by small vessel dysfunction in the liver and kidney (Stam, Kothari, *et al*, unpub. data). Further details are summarized below.

Ophthalmologic abnormalities

Changes to the retinal vasculature manifest between the fourth and sixth decades of life (mean age at presentation = 45). Retinal findings are progressive. Initially, these include telangiectasias, microaneurysms and cotton wool spots, but more severe disease shows a lack of capillary perfusion particularly around the fovea, eventually progressing to frank ischemia. Neovascularization of the retinal disc may also occur. Vitreous hemorrhage may occur associated with neovascularization (5) While some of the retinal vascular changes in these patients are visible on fundoscopic examination, the best visualization of the retinal changes is obtained using fluorescein angiography. Retinal fluorescein angiograms demonstrate capillary dropout, especially in the macula, leading to loss of central vision, telangiectasias and juxtafoveolar capillary obliteration (5, 20). Consequently, an ophthalmological consultation is valuable in patients suspected to have the disease. Although the ophthalmologic symptoms and retinal findings may precede other symptoms, neurological manifestations are usually demonstrated in parallel (5).

Neurologic abnormalities

Patients can present with a multitude of neurologic findings. Headaches are common along with focal neurologic deficits (most commonly motor deficits > sensory deficits > cerebellar deficits). Various psychiatric disturbances have also been noted including depression, personality changes and anxiety (Stam, *et al*, unpub. data). In some cases, the focal deficits and radiological appearance have been interpreted initially as a brain tumor (27). As with ocular abnormalities, the neurological symptoms are gradually progressive related to ongoing neurologic injury. Patients experience a slow, progressive cognitive deterioration including memory impairment in more advanced stages of the illness (Stam, *et al*, unpub. data). Eventually, all succumb from progressive neurologic decline.

MRI or computed tomography (CT) is useful in establishing the neurological involvement of the disease (Figure 1). Early changes that can be seen in individuals without focal neurological deficits include focal punctate calcifications, focal non-enhancing T2 hyperintense lesions in the periventricular and deep white matter, or post-contrast enhancing lesions of varying size and pattern similar to what is seen in symptomatic patients (Stam, *et al*, unpub. data). Among individuals with neurological symptoms, two patterns of MRI abnormalities have been reported. These include multiple focal areas of T2 hyperintensity in periventricular and deep white matter, as well as post-contrast enhancing pseudotumors of variable size. The latter are found in most patients

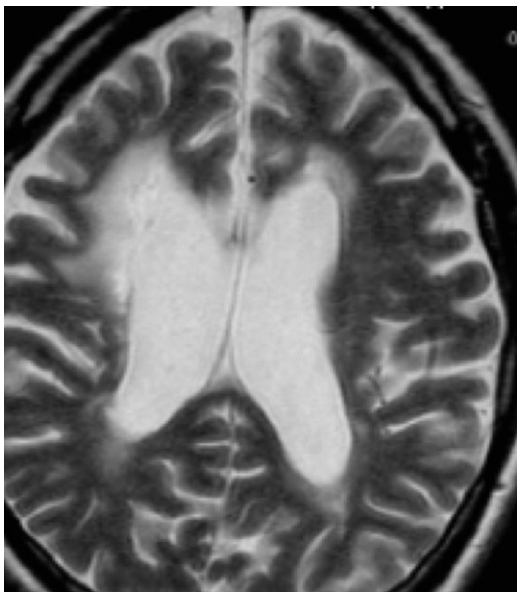

Figure 1. T2 weighted MRI from HERNS patient. MRI demonstrates elevated periventricular signal with enlargement of the lateral ventricles and cortical sulci.

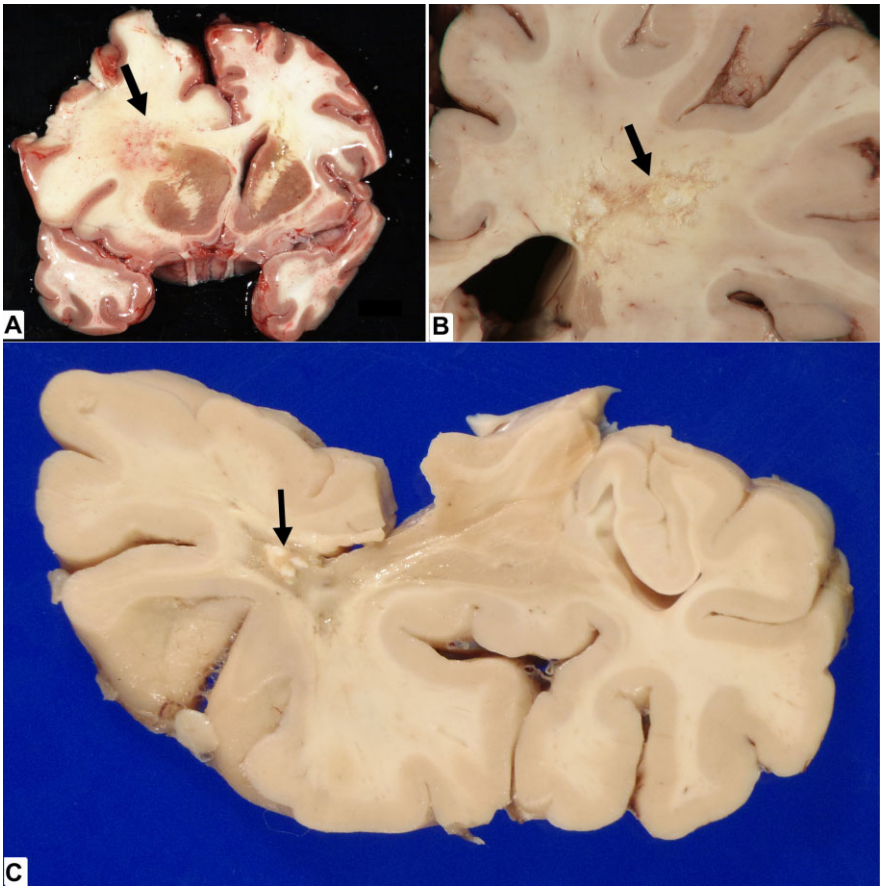

Figure 2. Gross appearance of lesions from CRV and HERNS patients. A. Fixed section demonstrates large space occupying lesion (arrow) in the left frontal lobe white matter and periventricular region. The lesion also involves portions of the deep gray nuclei and obliterates the left lateral ventricle, expands the cortical sulci and causes a midline shift. B. Fixed section from right parietal lobe of the same patient shows a separate periventricular white matter lesion (arrow) with central cores of white, firm parenchyma surrounded by a soft, translucent region consistent with the appearance of an infarct. The gray matter is spared. C. Fixed section from a left half coronal section at the level of the hippocampus from a HERNS patient showing a periventricular lesion (arrow) composed of a soft, translucent lesion with central punctate cores of white, firm parenchyma.

with clinical neurological symptoms. The pseudotumors are usually solitary but can be quite large with displacement of normal brain structures (disruption of sulci, midline shifts, etc.). They may display T1 hypointensity as well as surrounding edema. The edema is variable over time and with steroid treatment. Diffusion restriction is seen in some imaging series, often in the central portion of the pseudotumor. This phenomenon suggests alterations to the small vessels. Hemorrhage is not seen but focal calcifications occur in half of patients with neurological symptoms (Stam, *et al*, unpub. data). The frontal lobes are most often involved with a nearly even divide between periventricular and subcortical locations. However, the corpus callosum is always spared. Rare instances of infratentorial involvement are seen.

PATHOLOGICAL FEATURES

Neuropathological abnormalities

The white matter of the frontal lobe as well as periventricular deep gray nuclei and white matter are the most commonly affected regions of brain. Rarely, infratentorial regions are involved. Although the external surface of the brain is typically normal in appearance, the optic nerves were involved in one case. On gross examination (Figure 2), multiple, often coalesced areas of the brain are soft with a gelatinous appearance, frequently with a central prominent white firm region within these areas. The cortical gray matter is conspicuously spared. Histopathology of the grossly evident lesions (Figures 3–5) in both biopsy and autopsy materials demonstrate multiple, often confluent foci of coagulation necrosis surrounded by reactive gliosis. Immunohistochemistry

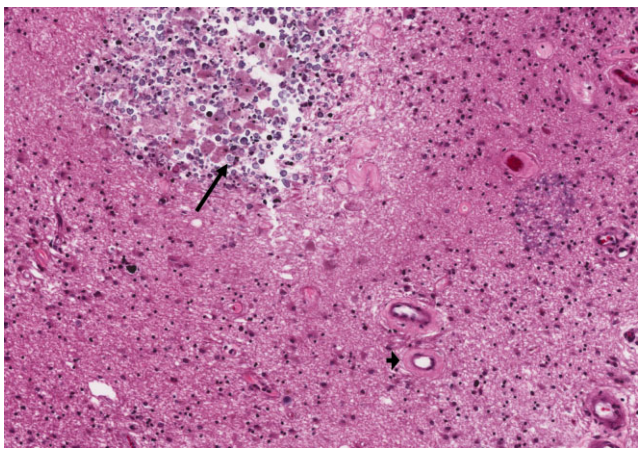

Figure 3. White matter from a CRV patient demonstrating astrocytosis, vascular hyalinization (arrowhead) and an infarct with a central region of dystrophic calcification (arrow).

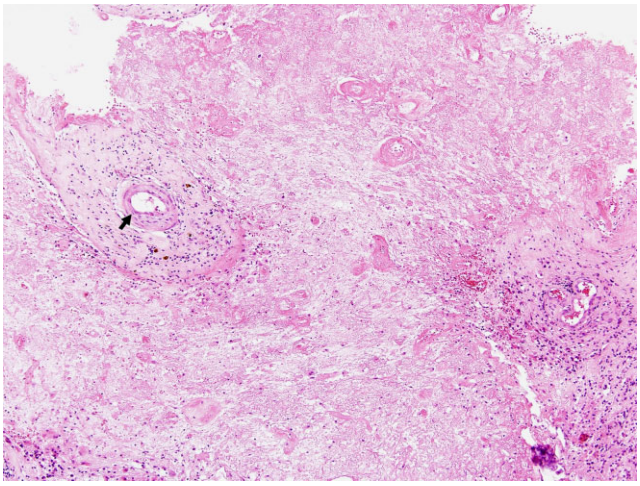

Figure 4. Ischemic white matter from a CRV patient demonstrates vascular wall hyalinization (arrow) with expanded adventitia. In some vessels, this is accompanied by increased numbers of inflammatory cells but vasculitic damage is not appreciated. A number of smaller vessels within the ischemic white matter are themselves necrotic.

for CD68 is particularly useful in highlighting extensive collections of microinfarcts that are otherwise not appreciated in H&E-stained sections. These can be multiple and quite subtle as the injury process appears to be ongoing. In some cases, neutrophils are seen in the surrounding parenchyma in larger lesions but this is inconsistent across the spectrum of HERNS and CRV cases studied. In the most advanced lesions, macrophages with foamy cytoplasm are seen corresponding to a chronic phase, and eventual cavitation of the involved white matter. Focal calcifications are seen most frequently associated with these regions. On biopsy, the characteristic appearance of these calcifications combined with abnormal vessel walls, though not pathognomonic of the disease, have, in our experience, been used to identify new cases from families unrelated to the known cohorts. In such circumstances, genetic testing for the mutations discussed below has confirmed the diagnosis.

The radiological differential diagnosis has often included an unusual case of multiple sclerosis (MS). Involvement of the deep white matter, particularly in the periventricular area, superficially mimics MS but the lesion seen histopathologically in CRV patients is more destructive than a demyelinating plaque of MS. Myelin loss is substantial in autopsy tissue; however, neurofilament immunolocalization also shows concomitant axon loss and, frequently, large numbers of swollen axonal spheroids, a pattern which is more consistent with a destructive rather than demyelinative process.

A striking vasculopathy of medium and small caliber parenchymal arteries as well as veins is usually noted within and adjacent to areas of the necrotic white matter. Currently, this is considered to be a fundamental aspect of the pathophysiology of the disease. The leptomeninges, extraparenchymal vasculature, and the cortical gray matter vessels are typically spared. In some cases, we have found inflammatory cells surrounding vessels (both CD45+ and CD68+ cells) that have less fibrosis, intact smooth muscle actin (SMA) staining layers and intact endothelial cells immunoreactive for CD31 (Figure 6). There is no evidence for a vasculitis, however, even in the context of these inflammatory cells. Rather, the morphological features consist of combinations of fibrinoid vascular necrosis, adventitial fibrosis, luminal narrowing and mural hyalinization seen throughout the tissue sections. In areas surrounding necrotic regions, vascular proliferation can be seen. Vascular thrombosis is rare but has also been noted in some autopsy reports. These latter two features correspond to the post-contrast enhancement that is sometimes seen by imaging within the lesions. Telangiectasias may be found but are a rare occurrence. It is important to note that there is no evidence of vascular amyloid deposition or of the extravascular granular Periodic acid-Schiff (PAS) positive deposits characteristic of CADASIL. The morphological features are most consistent with those seen in radiation necrosis, where areas of ischemia are punctate with vessels demonstrating fibrinoid vascular necrosis. CRV patients, however, do not have histories of radiation. In the past, the surrounding astrocytosis has been misdiagnosed in some individuals as a neoplastic process; however, further studies of these families have demonstrated that this process is clearly reactive. As discussed above, radiological data have at times been interpreted as an atypical form of MS, but neurofilament loss in addition to myelin loss rather strongly supports an ischemic process. Various other pathologies, including but not limited to infections, may also be seen overlying the CRV pathology because of previous attempts to treat these patients with high dose steroids targeting the cerebral edema. These treatment modalities have not been shown in the long term to slow the disease but in some cases have been used to decrease symptoms from edema.

Ocular pathology

Histopathological changes in the eye correspond to those seen by direct retinal examination. Although difficult to find in cross sections, epiretinal vessels with thickened, hyalinized walls can be visualized in some patients. Most often, in patients with more advanced retinal disease, necrotic changes to the nerve fiber, ganglion cell and inner nuclear layers are often noted. In less severe cases, scattered microinfarcts and cytoid bodies (in nerve fiber layer) can be seen. Other rarer epiretinal vascular changes include telangiectasias and fibrin thrombi. The choroidal vasculature and the photoreceptor layer of the retina are not affected. The latter raises the possibility that it is predominantly vasculature with tight junctions that is involved in the disease.

Other organ pathology

Some patients have had transaminase as well as cholestatic enzyme abnormalities. Histopathological examination of the liver in a significant number of patients showed regions of atrophic hepatocytes and parenchymal collapse alternating with compensatory hypertrophy, consistent with nodular regenerative hyperplasia (NRH). In addition to NRH, smooth muscle actin as well as CD34 immunohistochemistry staining patterns reflected capillarization of the sinusoids in some cases. Many patients, irrespective of a history of alcohol abuse, had some degree of hepatic fibrosis.

Renal insufficiency was frequent (75% with elevated CK in the CRV and HERNS cohorts) (Stam *et al*, unpub. data).

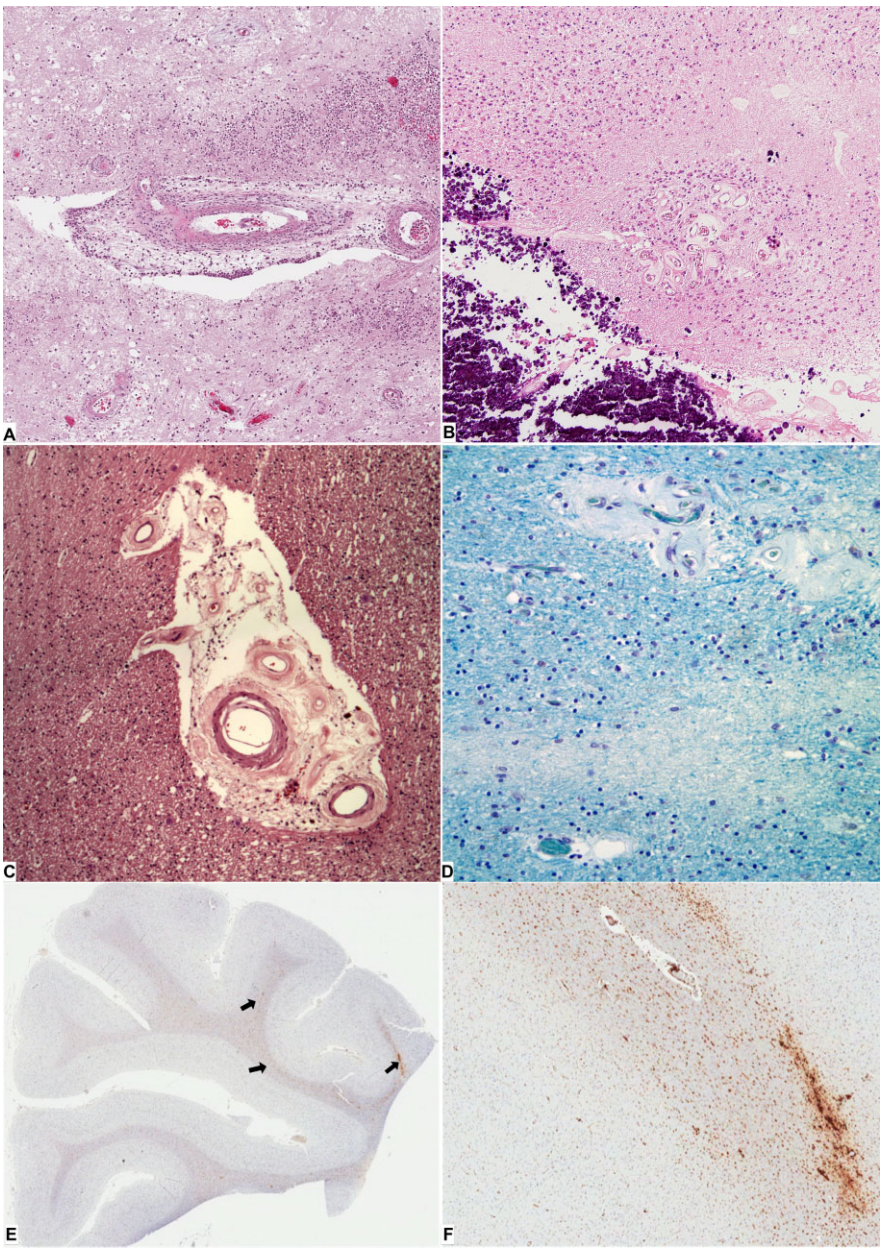

Figure 5. Vascular and white matter lesion in HERNS and CRV. A. A CRV patient demonstrating a moderately sized vessel with fibrinoid vascular necrosis. In the surrounding region, there is an influx of neutrophils consistent with a recently necrotic lesion. B. Reactive astrocytosis is seen in the white matter of a CRV patient adjacent to a region of dystrophic calcifications (seen at lower left). A vascular telangiectasia is also adjacent to the dystrophic calcifications. C. A cluster of vessels from a HERNS patient demonstrate significant hyalinosis of the wall along with adventitial fibrosis. D. A luxol fast blue stain of a region of white matter in a HERNS patient demonstrates focal regions of demyelination that also correspond to areas of neurofilament absence (by IHC), consistent with microscopic ischemic foci. E. Overview of the white and gray matter distribution of CD68 in a HERNS patient demonstrating a patchy, exclusively white matter distribution. F. A magnified view of the same section (as E) demonstrating a population of macrophages within one of the small ischemic foci in the white matter.

The cortical surfaces of the kidneys were frequently scarred. Renal histopathology was dominated by diffuse arterialopathies (arteriolonephrosclerosis, glomerulosclerosis). Fewer patients were seen with microthrombi and arteriosclerosis. The glomerular and arteriolar changes were seen irrespective of clinical evidence of hypertension.

Ultrastructural pathology

Ultrastructural changes have been examined in individuals from HERNS (8), CRV (Stam *et al*, unpub. data) and HVR cohorts (Stam *et al*, unpub. data). The predominant common feature remains a multilaminated basement membrane composed of alternating lamina densa and lamina lucida. Not all vessels demonstrate this change.

We compared grossly normal areas with those bordering coagulative necrosis in an untreated individual with CRV (tissue collected within 3 h of death; Figure 7). The changes in the vasculature of the brain reflected those noted by light microscopy. The lumens of the vessels in both necrotic and bordering areas were narrowed because of edematous endothelial cells (average thickness of 1.3 micrometers), compared with grossly normal areas (0.35 micrometers). Discontinuities in the lamina densa were noted but were rare. Endothelial cells from edematous areas bordering necrotic regions had increased secondary and autophagic lysosomes. In some cases, cytoplasmic blebs had formed on the lumenal surface of endothelial cells.

Collagen fibrils, consistent with types I and III, were deposited in thick, disorganized arrangements between the lamina densa and

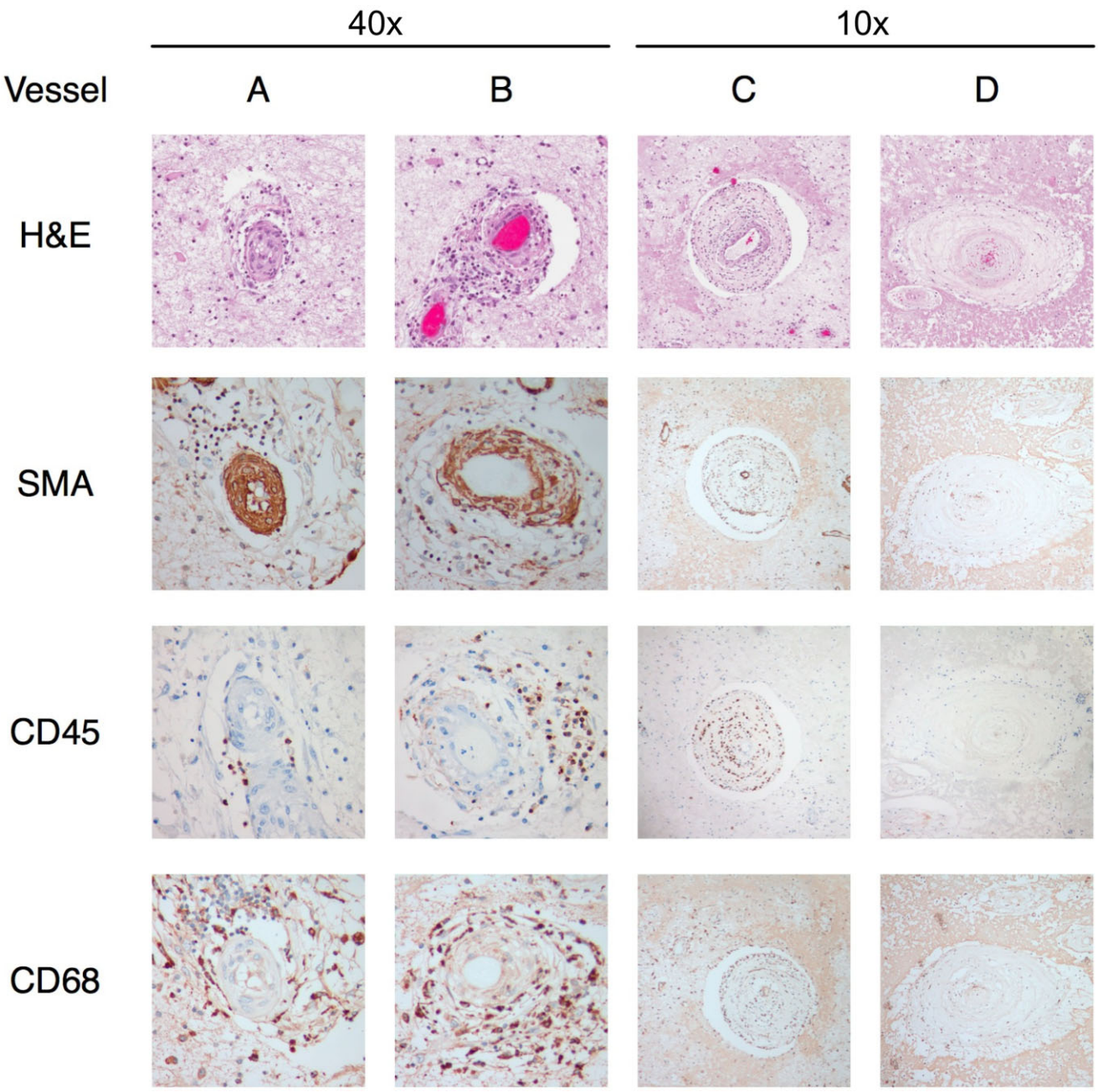

Figure 6. Vascular phenotypes seen within the white matter of CRV patients. The morphology of the vasculature in CRV patients differs with proximity to ischemic lesions. Thickening in the vessel walls is common. In some cases, the wall has cellular elements consisting of smooth muscle cells and occasional CD68+ cells (vessels A and B). In these, few CD45+ cells are seen. In other regions, often bordering regions of ischemia (vessel C), the amount of immunostaining of smooth muscle actin and CD68 is decreased. Increased CD45+ cells are seen in some of these vessels. Elsewhere, impressive adventitial thickening can be seen with evidence of loss of lumen integrity (RBC leaking) particularly within regions of ischemia (vessel D). These vessels show no definite cellular elements in their walls.

the external vessel boundary. Interspersed among and between collagen fiber bundles were cellular processes of pericytes or fibrocytes in greater frequency than in normal areas of the brain. The pericyte cytoplasm had more density than in normal areas; and autophagic granules, swollen mitochondria and distended rough endoplasmic reticulum were observed. In comparison, the normal areas of the brain did not have these thick deposits of collagen and the collagen present was organized in ordered bundles.

The basement membrane (including lamina densa and lamina lucida) of the endothelial cells in and bordering lesions was notice-

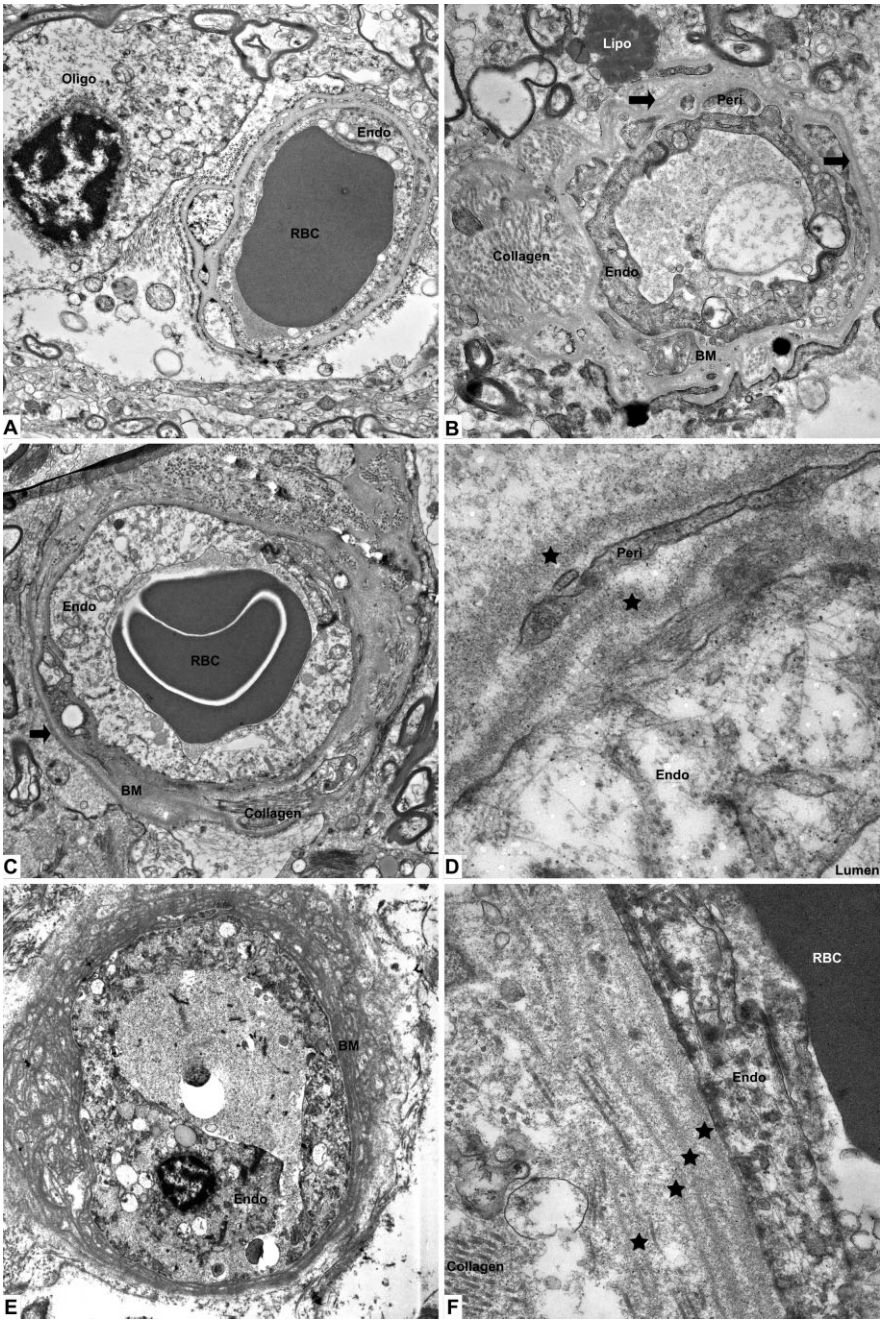

Figure 7. Vascular ultrastructure of the brain and kidney in CRV patients. Ultrastructure of the vasculature from various regions of the brain (panels A to D) and kidney (panel E and F) of an untreated patient collected within 3 h of death demonstrated striking changes in vascular morphology. A. A region of grossly normal appearing brain demonstrated vessels with normal appearing basement membrane, thin endothelial cells and a patent lumen. The surrounding parenchyma of the brain demonstrated unremarkable neuropil and cellular elements. B. A region bordering an ischemic lesion showed changes to the collagen layers surrounding vessels including increased layers of collagen and a basement membrane that shows thickening and regions with more than one lamina densa layer (examples at arrows). The endothelial cells also demonstrated increased vesicles and had coarse cytoplasm. The surrounding neuropil contains regions with increased lipofuscin and the pericyte foot processes surrounding the vessels have darker, dense cytoplasm. C. A vessel taken within a lesion demonstrates much thicker basement membrane material with entrapped collagen pockets and regions with duplicated lamina densa (arrows). The endothelial cells in this region are far thicker than in grossly normal areas. D. Higher magnification of a vessel wall from the brain showing duplicated lamina densa (stars). A pericyte foot process demonstrates darkened cytoplasm. E. Vessels from the kidney of a different patient show areas with multilaminated basement membranes consisting of alternating lamina densa and lamina lucida. F. A higher magnification of a vessel from the kidney demonstrates multiple layers of lamina densa (stars). Abbreviations: Oligo = oligodendrocyte; Endo = endothelial cell; RBC = erythrocyte; Lipo = lipofuscin; Peri = pericyte; BM = basement membrane.

ably thicker (1102 nm +/− 523 nm) but less electron dense than in non-lesional vessels (244 nm +/− 71 nm). In the capillaries and smaller arterioles of the lesion, only a single lamina densa was observed; however, in larger vessels, the thicker lamina densa had alternating electron dense and lucent areas producing a multi-laminated appearance.

Oligodendrocytes, microglia and neuronal synapses were noted throughout the neuropil of normal brain but the neuropil of areas adjacent to the lesion showed axon loss. Even in apparently normal areas, the astrocyte processes surrounding vessels appeared edematous, while in ischemic areas, they had a "watery" cytoplasm. Lipofuscin deposits, some filling the cytoplasm of microglia, were common.

Within the kidney, electron microscopy showed thickened capillary basement membranes (422 nm +/− 81 nm compared with normal thicknesses of 310–340 nm) but no podocyte effacement or patterns associated with the deposition of immunoglobulins or complement. Some interlobular arteries in the cortex showed duplicated lamina densa similar to that seen in arterioles in the brain. Splitting and lamellations in the glomerular basement

membrane suggested possible matrix remodeling. We were able to compare the renal pathology 8 years apart in the course of the disease in one patient. The histological features were similar between the early and terminal time points, differing only in features of chronicity.

Multilaminated membranes have also been noted in the skin of individuals with HERNS/CRV (8), a finding that has the potential for the basis of a nongenetic screening test.

GENETIC FEATURES

In 2001 a linkage analysis (17) mapped CRV, HERNS and HRV to 3p12.1-p21.3. Several years later in 2007, haplotype combination and sequencing of genes in the narrowed search region from nine RVCL families (CRV, HVR and HERNS) showed a distinctive set of mutations in the most abundant mammalian 3'-5' DNA exonuclease called the TREX1 (22). Exonucleases hydrolyze the phosphodiester backbone at the ends of the DNA strand. TREX1 in particular has an affinity for single-stranded deoxyribonucleic acid sequences, and has a highly hydrophobic carboxyl terminal region that is responsible for proper intracellular localization.

TREX1 is known to be part of the SET complex and is associated with the endoplasmic reticulum (1). Upon production of granzyme A superoxide, which is a non-caspase mediator of cell death (12, 13), TREX1 translocates to the nucleus with the rest of the SET complex, where its exonuclease activity helps to maintain immunological tolerance as a negative regulator of interferon stimulatory DNA (ISD) responses (1, 24). TREX1 tends to act on single-stranded DNA polynucleotide species that can be generated during the processing of aberrant replication intermediates. These intermediates are formed during normal transcription and replication (for instance, caused by stalling of DNA polymerases on regions of DNA that are damaged or repetitive in a sequence), but can also be formed because of DNA viruses including endogenous retroviruses (24), which account for nearly 10% of the genome. Single-stranded replication intermediates that lack proper processing by TREX1 can accumulate and lead to improper immunostimulation. The phenotype resulting from TREX1 deficiency presents as a chronic inflammatory disease (30). TREX1 knockout mice demonstrate systemic inflammation and die from an inflammatory cardiomyopathy (14). TREX1 is an important negative regulator of macrophage responses (18). Furthermore, it has been shown that HIV will not as effectively evade the immune system when mutations in the exonuclease domains of TREX1 are present (19, 29).

Mutations in TREX1 are implicated in several diseases besides CRV, including Aicardi-Goutieres syndrome (3), familial chilblain lupus (10, 21) and a small percentage of systemic lupus erythematosus patients (11, 15). In most of these diseases, mutations to the exonuclease domains of TREX1 (the enzymatically active site) result in an autoimmune phenotype. A few carboxyl terminal mutations also occur in SLE patients but do not result in the same frameshifts seen in HERNS/CRV.

In HERNS/CRV, and the related family of diseases, most of the frameshift mutations (Table 1) lead to a premature stop codon (22) and result in a truncated protein lacking 40–80 amino acids of its carboxyl-terminus, including a putative transmembrane region. Two known mutations create an extra-long reading frame but the function of the additional amino acids is unknown. Unlike the normal TREX1 protein, which is located in the perinuclear region consistent with the endoplasmic reticulum of resting cells, this mutant form of TREX1 is diffusely present in the cytoplasm and nucleus (22). Given what is known to date about the physiological role and regulation of the 3′-5′ DNA exonuclease activity of TREX2 (4, 7, 23), the implications of such an enzyme untethered to its normal localization raise numerous possibilities for its role in DNA damage or dysregulation of cellular responses. A primary focus of the current research is understanding the aberrant behaviors of truncated TREX1 mutant proteins and how this impacts DNA repair, inflammatory responses, vascular pathology and ultimately tissue damage.

Table 1. Current known frameshift mutations in CRV and HERNS patients.

Frameshift mutation	Deleted (–) or added (+) amino acids
V235fs	–74
T236fs	–74
T249fs	–52
R284fs	+11
L287fs	+11

Over the last several years, there has been some progress in understanding the primary cell types impacted by HERNS/CRV mutations in TREX1 in the brain. A polyclonal antibody to TREX1 has been developed that recognizes both the mutant as well as the normal protein (9). This antibody was used to identify CD68+ and Iba1+ cells with morphology consistent with microglia as the primary cell type in the brain expressing TREX1 (9). This finding implies that TREX1 may be directly or indirectly involved in alterations of an inflammatory response in CRV patients. Stellate, ramified and foamy cell forms of microglia (and in the case of the latter possibly macrophages) were all identified in CRV brain tissue and varied with frequency based on the distance from lesions (9). The localization of TREX1+ microglia (a subset of total microglia) in morphologically normal areas of the brain differed significantly between genetically normal individuals (including those who had suffered stroke) and brains from individuals with CRV (9). Consequently, a subset of microglia (TREX1 positive) has aberrant localization in CRV patients even without changes to cellular morphology to suggest activation.

SUMMARY

HERNS/CRV, now recognized together through the common molecular mechanism of TREX1 frameshift mutations, is a vasculopathy presenting in middle age with a short course to mortality (~10 years). The current understanding of the clinical manifestations of the disease centers around brain and ocular pathophysiological processes including aberrant basement membrane and extracellular matrix structure in small- to intermediate-sized vessels mimicking the changes seen in radiation damage. Frameshift mutations in the 3′-5′ exonuclease (TREX1) result in mislocalization of the protein involved in granzyme A-mediated apoptosis and protection against autoimmune surveillance. While the mechanism of vascular damage itself remains undetermined, the aberrant localization of TREX1 expression in a subset of

microglia suggests a broader immunological anomaly that manifests primarily as a vasculopathic process.

ACKNOWLEDGEMENTS

We are deeply grateful to Dr. John Atkinson for his clinical insights on the Saint Louis cohort of CRV patients and sharing his unpublished data. We also are grateful to Dr. Helen Liapis for the contribution of the EM image from the kidney vessel in a CRV patient. H.V.V. supported in part by P50 AG16570 and P01 AG12435.

REFERENCES

1. Chowdhury D, Beresford PJ, Zhu P, Zhang D, Sung J-S, Demple B *et al* (2006) The exonuclease TREX1 is in the SET complex and acts in concert with NM23-H1 to degrade DNA during granzyme A-mediated cell death. *Mol Cell* **23**:133–142.
2. Cohn AC, Kotschet K, Veitch A, Delatycki MB, McCombe MF (2005) Novel ophthalmological features in hereditary endotheliopathy with retinopathy, nephropathy and stroke syndrome. *Clin Experiment Ophthalmol* **33**:181–183.
3. Crow YJ, Hayward BE, Parmar R, Robins P, Leitch A, Ali M *et al* (2006) Mutations in the gene encoding the 3"-5" DNA exonuclease TREX1 cause Aicardi-Goutières syndrome at the AGS1 locus. *Nat Genet* **38**:917–920.
4. Dumitrache LC, Hu L, Hasty P (2009) TREX2 exonuclease defective cells exhibit double-strand breaks and chromosomal fragments but not Robertsonian translocations. *Mutat Res* **662**:84–87.
5. Grand MG, Kaine J, Fulling K, Atkinson J, Dowton SB, Farber M *et al* (1988) Cerebroretinal vasculopathy. A new hereditary syndrome. *Ophthalmology* **95**:649–659.
6. Gutmann DH, Fischbeck KH, Sergott RC (1989) Hereditary retinal vasculopathy with cerebral white matter lesions. *Am J Med Genet* **34**:217–220.
7. Jani D, Lutz S, Hurt E, Laskey RA, Stewart M, Wickramasinghe VO (2012) Functional and structural characterization of the mammalian TREX-2 complex that links transcription with nuclear messenger RNA export. *Nucleic Acids Res* **40**:4562–4573.
8. Jen J, Cohen AH, Yue Q, Stout JT, Vinters HV, Nelson S, Baloh RW (1997) Hereditary endotheliopathy with retinopathy, nephropathy, and stroke (HERNS). *Neurology* **49**:1322–1330.
9. Kothari PH (2014) Studies on the mislocalized exonuclease TREX1 that causes a systemic vasculopathy. Doctoral dissertation, Washington University in St. Louis.
10. Lee-Kirsch MA, Chowdhury D, Harvey S, Gong M, Senenko L, Engel K *et al* (2007) A mutation in TREX1 that impairs susceptibility to granzyme A-mediated cell death underlies familial chilblain lupus. *J Mol Med* **85**:531–537.
11. Lee-Kirsch MA, Gong M, Chowdhury D, Senenko L, Engel K, Lee Y-A *et al* (2007) Mutations in the gene encoding the 3"-5" DNA exonuclease TREX1 are associated with systemic lupus erythematosus. *Nat Genet* **39**:1065–1067.
12. Martinvalet D, Dykxhoorn DM, Ferrini R, Lieberman J (2008) Granzyme A cleaves a mitochondrial complex I protein to initiate caspase-independent cell death. *Cell* **133**:681–692.
13. Martinvalet D, Zhu P, Lieberman J (2005) Granzyme A induces caspase-independent mitochondrial damage, a required first step for apoptosis. *Immunity* **22**:355–370.
14. Morita M, Stamp G, Robins P, Dulic A, Rosewell I, Hrivnak G *et al* (2004) Gene-targeted mice lacking the Trex1 (DNase III) 3"→5" DNA exonuclease develop inflammatory myocarditis. *Mol Cell Biol* **24**:6719–6727.
15. Namjou B, Kothari PH, Kelly JA, Glenn SB, Ojwang JO, Adler A *et al* (2011) Evaluation of the TREX1 gene in a large multi-ancestral lupus cohort. *Genes Immun* **12**:270–279.
16. Niedermayer I, Graf N, Schmidbauer J, Reiche W (2000) Cerebroretinal vasculopathy mimicking a brain tumor. *Neurology* **54**:1878–1879.
17. Ophoff RA, DeYoung J, Service SK, Joosse M, Caffo NA, Sandkuijl LA *et al* (2001) Hereditary vascular retinopathy, cerebroretinal vasculopathy, and hereditary endotheliopathy with retinopathy, nephropathy, and stroke map to a single locus on chromosome 3p21.1-p21.3. *Am J Hum Genet* **69**:447–453.
18. Pereira-Lopes S, Celhar T, Sans-Fons G, Serra M, Fairhurst A-M, Lloberas J, Celada A (2013) The exonuclease Trex1 restrains macrophage proinflammatory activation. *J Immunol* **191**:6128–6135.
19. Pontillo A, Girardelli M, Catamo E, Duarte AJ, Crovella S (2013) Polymorphisms in TREX1 and susceptibility to HIV-1 infection. *Int J Immunogenet* **40**:492–494.
20. Qian Y, Kosmorsky G, Kaiser PK (2007) Retinal manifestations of cerebroretinal vasculopathy. *Semin Ophthalmol* **22**:163–165.
21. Rice G, Newman WG, Dean J, Patrick T, Parmar R, Flintoff K *et al* (2007) Heterozygous mutations in TREX1 cause familial chilblain lupus and dominant Aicardi-Goutieres syndrome. *Am J Hum Genet* **80**:811–815.
22. Richards A, van den Maagdenberg AMJM, Jen JC, Kavanagh D, Bertram P, Spitzer D *et al* (2007) C-terminal truncations in human 3"-5" DNA exonuclease TREX1 cause autosomal dominant retinal vasculopathy with cerebral leukodystrophy. *Nat Genet* **39**:1068–1070.
23. Smith CG, Naven M, Harris R, Colley J, West H, Li N *et al* (2013) Exome resequencing identifies potential tumor-suppressor genes that predispose to colorectal cancer. *Hum Mutat* **34**:1026–1034.
24. Stetson DB, Ko JS, Heidmann T, Medzhitov R (2008) Trex1 prevents cell-intrinsic initiation of autoimmunity. *Cell* **134**:587–598.
25. Storimans CW, Oosterhuis JA, Van Schooneveld MJ, Bos PJ, Maaswinkel-Mooy PD (1990) Familial vascular retinopathy. A preliminary report. *Doc Ophthalmol* **75**:259–261.
26. Terwindt GM, Haan J, Ophoff RA, Groenen SM, Storimans CW, Lanser JB *et al* (1998) Clinical and genetic analysis of a large Dutch family with autosomal dominant vascular retinopathy, migraine and Raynaud's phenomenon. *Brain* **121** (Pt 2):303–316.
27. Weil S, Reifenberger G, Dudel C, Yousry TA, Schriever S, Noachtar S (1999) Cerebroretinal vasculopathy mimicking a brain tumor: a case of a rare hereditary syndrome. *Neurology* **53**:629–631.
28. Winkler DT, Lyrer P, Probst A, Devys D, Haufschild T, Haller S *et al* (2008) Hereditary systemic angiopathy (HSA) with cerebral calcifications, retinopathy, progressive nephropathy, and hepatopathy. *J Neurol* **255**:77–88.
29. Yan N, Cherepanov P, Daigle JE, Engelman A, Lieberman J (2009) The SET complex acts as a barrier to autointegration of HIV-1. *PLoS Pathog* **5**:e1000327.
30. Yang Y-G, Lindahl T, Barnes DE (2007) Trex1 exonuclease degrades ssDNA to prevent chronic checkpoint activation and autoimmune disease. *Cell* **131**:873–886.